Applied Thermal Engineering 75 (2015) 93–102

Contents lists available at ScienceDirect

Applied Thermal Engineering

journal homepage: www.elsevier.com/locate/apthermeng

Assessment of the EDC combustion model in MILD conditions with in-furnace experimental data

Delphine Lupant*, Paul Lybaert

University of Mons, Research Institute for Energy, Thermal Engineering and Combustion Unit, Rue de l'épargne 56, B-7000 Mons, Belgium

HIGHLIGHTS

- An experimental data set is generated in a laboratory scale MILD furnace.
- RANS simulations is done with ANSYS Fluent with two combustion models.
- The improvement brought by the EDC model in MILD conditions is shown.
- The sensitivity of the EDC model needs further investigation to be validated.

ARTICLE INFO

Article history:
Received 25 October 2013
Accepted 10 October 2014
Available online 17 October 2014

Keywords:
MILD combustion
Experimental
Detailed in-furnace measurements
Turbulence-chemistry interaction
Eddy-Dissipation concept

ABSTRACT

The paper presents a detailed experimental data set in a MILD combustion furnace. This laboratory scale furnace was especially designed to combine a small computational time with a kind of industrial operation. The in-furnace measurements are compared to the numerical results obtained with two turbulence–chemistry interaction models: the Eddy-Dissipation Model (EDFR) and the Eddy-Dissipation Concept (EDC). It is confirmed that the EDC model brings interesting improvements, compared to the EDFR model. First, it improves the prediction of the NO_x emission thanks to the possibility to include in the reaction mechanism some radical species required to compute the NO reaction rates. Then, this model is able to capture the kinetic limitation responsible for the reaction delay and which impacts the reaction progress through the furnace. The effect of the operating conditions is correctly reproduced in a relative way, what is not the case with the EDFR model. However, due to its high sensitivity to the operating conditions the EDC model is not able to reproduce the shape and the position of the reaction zone with precision. In conclusion, the EDC model still needs to be optimized for MILD combustion modelling and requires detailed experimental data to this end, as proposed in this paper.

1. Introduction

MILD combustion [1] offers the possibility to combine low pollutant emission with higher energy efficiency. This combustion technique was first named as flameless combustion by Wunning and Wunning [2] or High Temperature Air Combustion (HiTAC) by Hasegawa et al. [3] in the end of the nineties. Since this moment a lot of work has been done on MILD combustion experimentally and numerically. Among the experimental approaches, we can find parametric studies which observe the effect of some parameters on the combustion process with global measurements, and detailed studies, giving a lot of measurements inside the reactive mixture, but often for a reduced number of operating conditions. Only the second approach is developed here under, by stressing on the use of the experimental data for the validation of the numerical modelling. MILD combustion is based on the massive recirculation of hot combustion products into the reactants. In their numerical study of a labscale furnace in MILD conditions, Tabacco et al. [4] clearly explain that the combination of the high dilution and the low temperature level, resulting from this recirculation, reduces significantly the reaction rates and makes the interaction between chemistry and turbulence more important. For the numerical modelling, it means that the turbulent–chemistry interaction is particularly important and that the fast chemistry assumption commonly used for classical flames is not suited in MILD conditions.

Detailed measurement together with assessment of several turbulence and combustion models have been proposed at different scales. Christo et al. [5] studied a jet in hot and diluted co-flow, the coflow representing the mixing between combustion air

* Corresponding author. Tel.: +32 65 37 44 98; fax: +32 65 37 44 00.
E-mail address: delphine.lupant@umons.ac.be (D. Lupant).

http://dx.doi.org/10.1016/j.applthermaleng.2014.10.027
1359-4311/

and recirculating combustion products. This open configuration is well suited for laser-based measuring instruments giving detailed information. It is also interesting for the numerical modelling since its configuration can be reduced to a 2-D axisymmetric model and allows the use of models more computationally demanding. Among the three turbulence k-ε models, it was found that a modified version of the standard k-ε gives the best agreement with experimental data. For the combustion, the single conserved-scalar based models failed to predict the distribution of temperature and species, since it does not take into account the kinetic limitation for the reaction, as mentioned by Tabacco et al. [4] showing the strong overestimation of temperature in MILD conditions with this kind of model. The Eddy-Dissipation Concept model (EDC) led to good numerical predictions especially with detailed chemistry. The Eddy-Dissipation Concept was also assessed on the Delft jet in hot coflow by De et al. [6] and validated against detailed measurements. In this case, it is the realizable k-ε model which is used for turbulence modelling since it performed better than the standard k-ε. An improvement of the EDC model is suggested by the authors by modifying the model constants because the lift-off height wad underestimated with the default values. Christo et al. [5] concluded, from their side, that for a lower oxygen content in the co-flow, the model overestimated the lift-off. It demonstrates that the model is not entirely satisfying in all cases.

On a much larger scale, Mancini et al. [7] proposed the validation of the turbulence and combustion models with in-furnace measurements in a 0.58 MW furnace equipped with a burner operating in steady-state conditions. The k-ε RNG turbulence model give better results than the standard or the realizable version of the k-ε model, what is contradictory with the observations of Christo et al. [5] and De et al. [6]. But the way the mixing between reactants occurs is different according to the configuration. As Wang et al. [8] mention in their numerical study of the jet in hot coflow configuration, the fuel jet and the diluted oxidant co-flow are mixed mainly by diffusion while, in industrial furnaces, the mixing is driven by turbulent convection due to the high level of flue gas recirculation. This large scale recirculation with high streamline curvature can explain why the k-ε RNG model performs better. About the combustion model, Mancini conclude again that the EDC with a skeletal reaction mechanism was the most satisfying model. Parente et al. [9] study the effect of the turbulence–chemistry interaction on an industrial recuperative burner, comparing a global Eddy-Dissipation/Finite Rate model with the EDC model combined with different reaction mechanisms. They found that only the EDC model with the detailed reaction mechanism was able to predict the correct level of NO emission. Danon et al. [10] also used the EDC model with a skeletal reaction mechanism to study the effect of the burner's configuration in a 300 kW furnace but validated the model setup with measurements at outlet only, due to the lack of in-furnace experimental data.

The advantage of the experimental tests at large scale is that the conditions in which combustion occurs are realistic, with internal recirculation at large scale, real burner design with jet interaction, and heat transfer to the walls and to a colder surface representing the load. In this case, however, measurements inside the furnaces are more difficult to implement. Moreover, the computational domain being larger, it reduces the level of detail for the numerical investigation due to computational resources limitations.

Detailed experimental data can also be found in the literature at an intermediate scale and level of complexity. Szego et al. [11] generated temperature field in a 15 kW furnace, with parallel jets injection and flue gas extraction on the same side, to study the performance and stability characteristics of MILD combustion. The recirculation is ensured by entrainment of the reactant jets and the load is featured with one water cooled tube asymmetrically positioned on the side wall. Fields of temperature inside a 20 kW furnace equipped with a regenerative burner are also presented by Sanchez et al. [12] to study the effect of the oxygen enrichment on the performance of a MILD combustor. In this case, the cooling tubes are fed with air. Very recently Roiha et al. [13] as well as Rebola et al. [14] experimentally study the MILD combustion in labscale furnaces, but without cooling device, so without a real control of the furnace temperature. The first, proposed to examine the effect of air preheating and recirculation level on the stability of MILD combustion. The recirculation is realized externally with a particular injection system without real jet interaction. The in-furnace measurements are available along one vertical and one horizontal line. The authors add a short numerical analysis using the k-ε realizable turbulence model with the Eddy-Dissipation model. Rebola et al. [14] worked on a top-down firing burner with a coflow injection system in a cylindrical combustion chamber. Detailed measurements of temperature and main species are realized for two operating conditions varying the thermal input, the excess air, the air preheating temperature and flue gas temperature at outlet. Castela et al. [15] published similar results but for an exhaust located on the same side as the injection system. A second paper from Rebola et al. [16] focus on the numerical modelling of one set of operating conditions presented in Ref. [14], with the aim to compare the performances of different turbulence and combustion models. They conclude that the k-ε standard model give slightly better results than the other turbulence models tested: the k-ε realizable, the k-ε RNG and even the Reynolds Stress Model. About the combustion model in itself, the EDC model perform best, with equivalent results for the temperature and the major species mole fractions obtained with all the reaction mechanisms tested. Only the CO was not satisfactory.

The main purpose of this paper is first to presents detailed in-furnace measurements of temperature and 5 different species mole fractions (CH_4, CO, CO_2, O_2, NO) in a 30 kW lab-scale furnace operating in MILD conditions. The injection system is made of high momentum convergent reactant jets and the furnace temperature is controlled by sliding water-cooled tubes featuring the load. Two sets of operating conditions are considered with all the parameters kept constant but the excess air. This results in a strong modification of the reaction progress in the furnace due to chemical kinetic limitation. This pair of experimental data set seems therefore of particular interest to assess the performances of combustion models like the Eddy-Dissipation Concept in MILD conditions. The secondary purpose of the paper is then to use this combustion model for the numerical modelling of the furnace and to highlight the potential improvement it brings to the predictions compared to the more simple and cost effective Eddy-Dissipation/Finite Rate model.

2. Experimental set up

The furnace is designed to perform detailed with operating parameters (gas power, air preheating temperature, flue gas temperature and excess air) varying independently over a large range. It is schematically represented in Fig. 1a. More details about the instrumentation represented on this schematic view can be found in Ref. [18]. The burner geometry is similar to the industrial NFK regenerative burner [21], it is simply made of three gas injections: one central air injection and two off-axis fuel injections. The furnace temperature is controlled thanks to four water-cooled tubes by varying their immersion in the combustion chamber. Flue gas is leaving the combustion chamber trough 12 orifices positioned on the top of the vertical walls.

It was decided to test two different sets of operating conditions each corresponding to one of the topologies identified in a previous

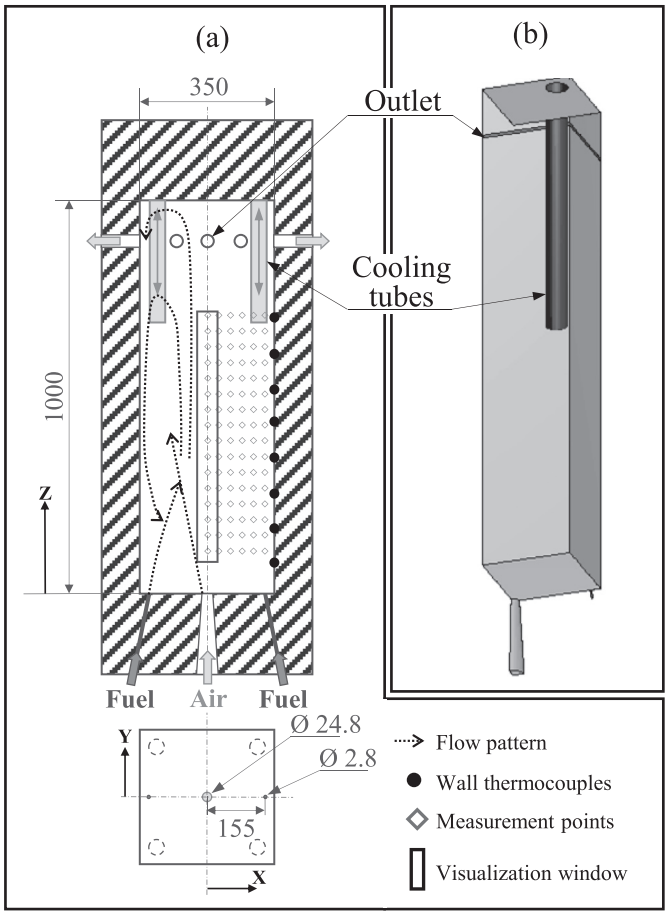

Fig. 1. Furnace (a) schematic and position of measuring instruments (units: mm); (b) computational geometry.

parametric study[17], based on the visualisation of OH self-emission in UV through the window represented on Fig. 1a. The standard topology is the most stable one with two zones in which heat release is maximum, called 'reaction zones' in the following, located at the meeting points between air and fuel jets. The low temperature topology is observed when decreasing the furnace temperature. In this case, heat is released along the air jet axis farther downstream as the furnace temperature keeps decreasing. The fuel is natural gas (fuel power 30 kW) with the following average volumetric composition: 0.8950 CH_4, 0.0548 C_2H_6, 0.0134 C_3H_8, 0.0046 C_4H_{10}, 0.0019 C_5H_{12}, 0.0158 N_2, 0.0145 CO_2 (lower heating value 37.2 MJ/m^{3}N). Air preheating temperature is fixed at 800 °C while the furnace temperature is kept around 1120 °C at the outlet. At this furnace temperature, the low temperature topology for a value of excess air equal to 10% is observed while for $E = 20\%$ the heat released distribution present a standard topology. In the following the value of E is used to refer to the one or the other topology for convenience.

3. Numerical method

3.1. Grid and computational domain

The computational domain is limited to the gas volume and reduced to one quarter of the furnace thanks to the symmetry. The external surface of the cooling tubes is modelled, so that 2 meshes were generated, one for each set of operating parameters. The outlet geometry was simplified by replacing the 12 orifices by a rectangular slit of equivalent area. The reference grid is unstructured and counts 340,000 hexahedral cells. The differences obtained on the numerical results by increasing the number of cells to 640,000 are not significant, so it was decided to keep the first one.

3.2. The models

Modelling is performed using 3-D RANS equation in steady state with ANSYS Fluent. The k-ε RNG model was chosen for the turbulence and the Discrete Ordinate model for the radiative heat transfer, for which the angular discretization is fixed to 16 solid angles per octant (4×4). The absorption coefficient is computed thanks the Weighted Sum of Grey Gases model, using the domain dimension to compute the characteristic length.

The main objective for the turbulence–chemistry interaction, is to test the Eddy-Dissipation Concept Model (EDC) [19]. This model was developed from the Eddy-Dissipation Model of Magnussen and Hjertager [20] to take into account chemical kinetic. The Eddy-Dissipation Concept supposes that the reaction occurs in fine turbulent structures for which the characteristic length and residence time are computed from turbulent quantities. Those structures are considered as perfectly stirred reactor in which the chemistry can be treated with detailed reaction mechanisms. The computational time largely increases with the number of species of the reaction mechanism. A compromise was found here by using the reaction mechanism for methane proposed by Smooke [21], including 17 species and 25 reactions, as it performs reasonably well in the numerical study of Christo et al. [5]. The Eddy-Dissipation model computes a turbulent reaction rate empirically from the local species content and the turbulent mixing time (ε/k), by assuming infinitely fast chemistry ("mixed-is-burnt" hypothesis). This model can only be applied with global reaction mechanisms such as the methane-air two step chosen in this study. A kinetic limitation can also be introduced by computing a laminar finite rate, and taking the minimum between kinetic and turbulent mixing rates. This combination is referred as the Eddy-Dissipation/Finite Rate (EDFR) in the following. It appears that this simplified model gives overestimation of the temperature (Parente et al. [9]) and wrong prediction of the CO mole fraction (Christo et al. [5]) in the near burner zone. EDC and EDFR are also compared in details by Rebola et al. for the simulation a co-flow configuration in a flameless combustor [16]. The EDFR model performs quite well, even if not better than the EDC in the near burner zone (that is in the fuel jet) because in this region the reaction is kinetically limited. However, the discrepancies are increasing downstream since the reaction becomes limited by the mixing with the EDFR and the chemical kinetic is not taken into account anymore. Some studies have shown that a modification of the Eddy-Dissipation model's constant A from 4 to 0.6 can give satisfactory results in MILD conditions. The value of $A = 0.6$ was found to be appropriate for the modelling of a 2.25 MW swirling natural gas flame by Peters et al. [22], based on temperature and main species profiles. Hekkens and Mancini [23] also obtained good results with the EDFR model and this value of A when modelling an IFRF facility equipped with an NFK type natural gas burner. In a previous study on the numerical simulation of an FLOX® natural gas burner in a semi-industrial scale furnace [24], this reduction of the constant was also found to improve the distribution of the temperature and the species inside the furnace, especially in the near burner zone. The reduction of the constant has the effect to reduce the reaction rate computed by the Eddy-Dissipation Model (mixing rate). On a more fundamental level, Zahirovi et al. [25] improved the performance of the EDFR model also by reducing the value A to 0.6 when modelling the Sandia Flame B, even if they conclude that the EDC model is the best option. This flame, fed with a fuel composition of 40% CO, 30% H_2 and

30% N_2 by volume, was considered by the authors to reflect the flue gas recirculating stream reacting with air in a biomass furnace.

A simple combustion model as the EDFR model with a constant tuned but giving reasonably good results in MILD conditions would be interesting since the computational cost is much lower compared to the EDC model. Indeed, the CPU time using the EDC model increases by a factor of about 15 compared to the numerical simulation with the EDFR model. For this reason, the EDFR model with adjustment of the constant A was also considered for the comparison with experimental data.

The NO_x production is computed in a post processing step considering 3 formation routes as implemented in ANSYS Fluent: the thermal route, the prompt route and the N_2O route, which is important at low temperature (<1800 K) and high pressure. The O and OH contents are required to compute the reaction rates of NO with the thermal and the N_2O routes. Those species are included in the reaction mechanism used with the EDC model, but have to be estimated with the EDFR from O_2 and H_2O content considering equilibrium. The turbulence–chemistry interaction is modelled thanks to a probability density function (β) on the temperature and the oxygen mass fractions.

3.3. Boundary conditions

Experimental measurements are used to fix the boundary conditions. Mass flow rates, temperature and species content of air and fuel jets are set at inlets. The outlet is set at atmospheric pressure. The average water temperature is imposed at the external surface of the cooling tubes and the emissivity is set to 0.5 to obtain an acceptable value for the heat transfer to the tubes. For the walls, the total heat loss from experimental heat balance is considered uniformly distributed on the walls, and used to deduce a global heat transfer coefficient between the inner wall temperature (average measured value) and the external environment temperature. The emissivity of the walls is fixed at 0.3, but its effect on the results is not significant.

4. Results and discussion

4.1. Flow pattern and fuel consumption

Since 90% of the natural gas volume is methane, this species was chosen as fuel marker. Methane content gives information about the fuel jet trajectories, obtained by locating the points at which its value is maximum for a given Z position. Fig. 2 presents those experimental trajectories, together with the flow pattern obtained from the numerical velocity field in plane (X,Z). The computed jet trajectory is the position of the maximum Z velocity in the jet area. The experimental trajectories are not completely symmetrical, since open squares and full squares representing the right-hand and the left-hand side trajectories, are not at the same positions. All the numerical trajectories are coincident but less bended towards the central air jet compared to the experimental values. The air jet radius is defined as the point where the Z velocity drops below to half its value along the jet centreline and the recirculation zone delimits the zone within which the Z velocity is negative. From those elements it is clear that the choice of the combustion model has not a strong influence on the flow field, so that the differences observed in the following are mainly due to the combustion model. The increase of the air flow rate with $E = 20\%$ does not change significantly the flow pattern either.

Fields of methane in plane (X,Z) can be used to observe experimentally the penetration of the fuel jets inside the furnace for both operating points (Fig. 3a). It can be seen that the fuel is slowly consumed since 0.2% of methane is still measured halfway up. For

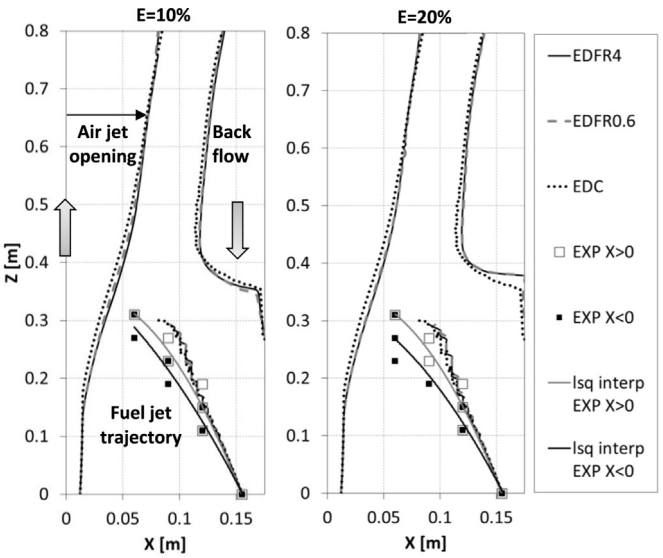

Fig. 2. Flow pattern: air jet opening, recirculation zone and fuel jet trajectory.

$E = 10\%$ methane is present along the air jet axis and farther downstream in comparison to the case $E = 20\%$, what means that the air jet entrains methane which is not yet oxidized for the lowest value of the excess air.

In Fig. 3b, the quality of the numerical prediction is first analysed from the iso-lines of CH_4 mole fraction. For a mole fraction of 1% (dry basis), the number of experimental points, obtained by linear interpolation, is high enough to capture the shape of the iso-line and the resulting observations are representative of the effect of the combustion model throughout the plane. Fig. 4 give additional information by presenting the measured and predicted profiles at three Z positions from the burner.

It is interesting to note that, on the left side of the fuel jet, the shape of the experimental iso-lines (symbols) on Fig. 3a and the CH_4 decrease on Fig. 4 are correctly reproduced especially with EDC (dotted lines). For all the combustion models the position of the curve at $Z = 0.15$ m where air and fuel jets begin to interact is well captured. It is not the case on the opposite side of the fuel jet where the computed iso-lines are nearly coincident, but too close to the wall (Fig. 3b), and the CH_4 mole fractions are too high compared to measurements (Fig. 4). Regarding this discrepancy together with the computed trajectory less bended towards the air jet, it reveals an interaction with the wall that is more important compared to the experiments, for which the recirculation flow seems to go deeper towards the bottom of the furnace.

The effect of the constant A with the EDFR models appears through the delay for the CH_4 consumption from EDFR (solid lines) to EDRF06 (dashed lines) but its impact is less significant than the use of the EDC (dotted lines). With the EDC model, the consumption of CH_4 is even slower, and is more sensitive to the operating conditions. On Fig. 4, for $E = 10\%$ and $Z = 0.43$ m, the EDC model predict 1% of CH_4 along the axis as expected from the measurements. This demonstrates that the EDC model is able to capture the delay introduced by chemical kinetics, unlike the EDFR0.6 model which reduces the reaction rate similarly for both operating points.

4.2. The reaction zone

The reaction zone means here the zone in which heat is released. It can be observed experimentally from the visualization of OH self-emission in UV [17], but this measurement is limited to

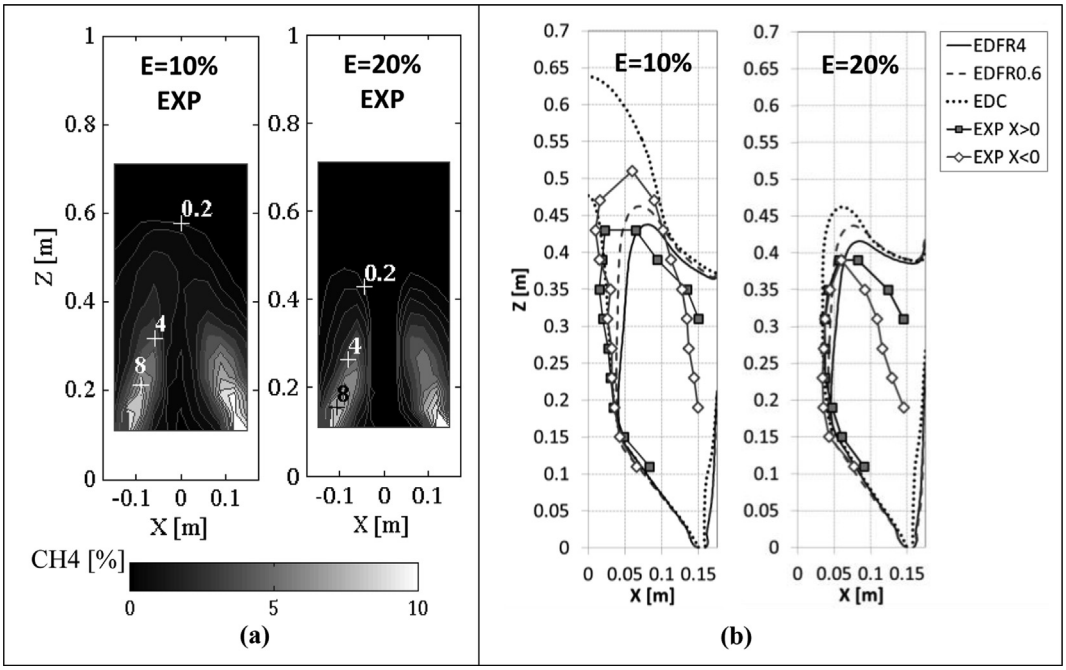

Fig. 3. (a) Experimental CH_4 mole fraction (dry basis) in plane (*X*,*Z*) (b) Comparison of iso-lines of 1% CH_4 (dry basis) with numerical results.

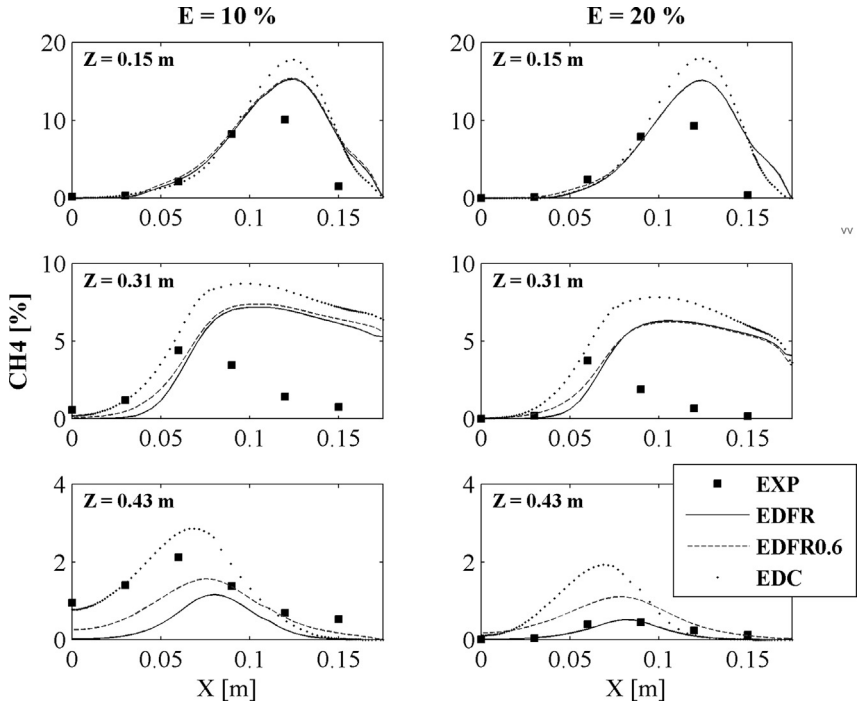

Fig. 4. Measured and predicted CH_4 molar fraction (dry basis) profiles obtained using different combustion models.

the window's opening (Fig. 1). On the other hand, the measurements of species content cover a wider zone inside the furnace and CO, as intermediate species, could be considered to observe globally the shape and the position of the reaction zone. This is checked in Fig. 5 by comparing the maximum of CO content and the maximum OH emission (I_{OH}) along the *Z* direction in a relative way. It is shown that the evolutions are similar, with just a small shift of the maximum of CO downstream in comparison with the maximum of OH. It is concluded that the CO distribution can be considered in the following to characterize what is called 'the reaction zone'.

4.2.1. Shape and position

The experimental CO distribution in plane (*X*,*Z*) can be observed in Fig. 6a for $E = 10\%$ and Fig. 7a for $E = 20\%$, by considering the reaction zone as the region where CO is present in high quantity.

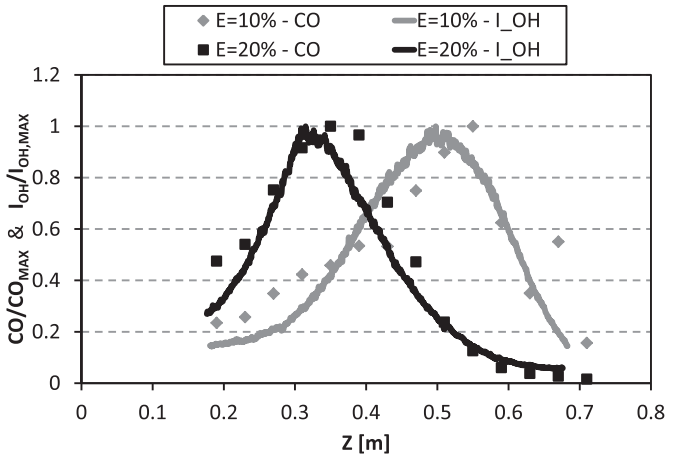

Fig. 5. Maximum of experimental CO content (dry basis) and OH emission (IOH) along *Z* axis.

As expected in MILD combustion, the reaction zones are extended on a large fraction of the investigated plane and the CO mole fractions are well below 1%, with a maximum around 3100 ppm for $E = 10\%$ and 6900 ppm for $E = 20\%$. The shape and position of the reaction zone for both operating points is consistent with the standard and low temperature topologies described in paragraph 2.

Looking then at the computed fields (Fig. 6b, c, d and Fig. 7b, c, d), it seems that any of the combustion models is able to reproduce those experimental CO distributions, especially for $E = 10\%$. With the EDFR model, the reaction occurs within very thin volumes between reactant jets for both operating points (Figs. 6b and 7b). For the highest value of *E*, the reaction occurs additionally on the edge of the fuel jets. The maximum value of the CO content does not change significantly by changing the excess air since it is equal to 4093 for $E = 10\%$ and 4358 ppm for $E = 20\%$. The reduction of the constant A with the EDFR model (EDFR0.6) has no effect on the position where the reaction is the more intense but spreads the reaction zone nearly over the entire furnace volume (Figs. 6c and 7c). Indeed, the zones in which the CO mole fraction is below 1000 ppm are reduced to the reactant jets. Even if it is a little higher, the maximum CO concentration does not change when increasing excess air as in the experiment. The change in the reaction zone topology with the value of *E* is actually observed only with the EDC model. For $E = 10\%$, the reaction zone is lifted downstream along the *Z* axis (low temperature topology), but too far from the burner compared to experiment (+0.25 m). Moreover its shape reveals that the reaction goes on in the recirculation zone along the walls towards the fuel jets, a fact which is not consistent with the experimental observations. By increasing *E* to 20%, two maxima of CO content (8,559 ppm) appear on both sides of the air jet axis, but around $Z = 0.5$ m, that is beyond the meeting point of the reactant jets. However, even if two maxima can be identified, iso-values of CO fraction form a single reaction zone below 6000 ppm whereas on the experimental field, it is clear that the CO content drops below 500 ppm between the two reaction zones in the vicinity of the air jet axis. The EDC model together with the Smooke mechanism [21] is able to detect a modification in the way the combustion proceeds by increasing the excess air, since the maximum CO concentration is nearly doubled and that the reaction zone is lifted downstream. However, the model predicts the position of this reaction zone too far downstream. The fact that the EDC model is able to correctly capture the delay introduced by chemical kinetics was also observed from CH_4 distribution, but this delay is too important if compared to experiment. This could be improved by changing the empirical constant of the model as it is done by De et al. [6] and

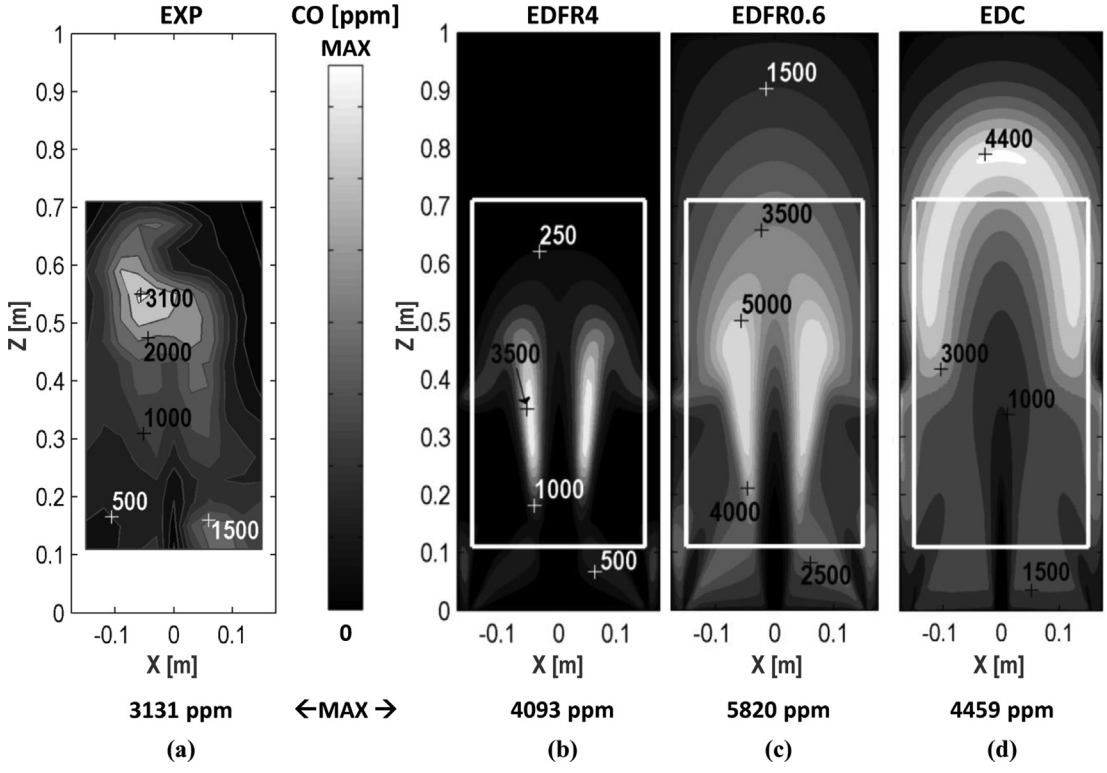

Fig. 6. Experimental (a) and numerical (b, c, d) CO mole fractions (dry basis) in plane (*X*,*Z*) for $E = 10\%$.

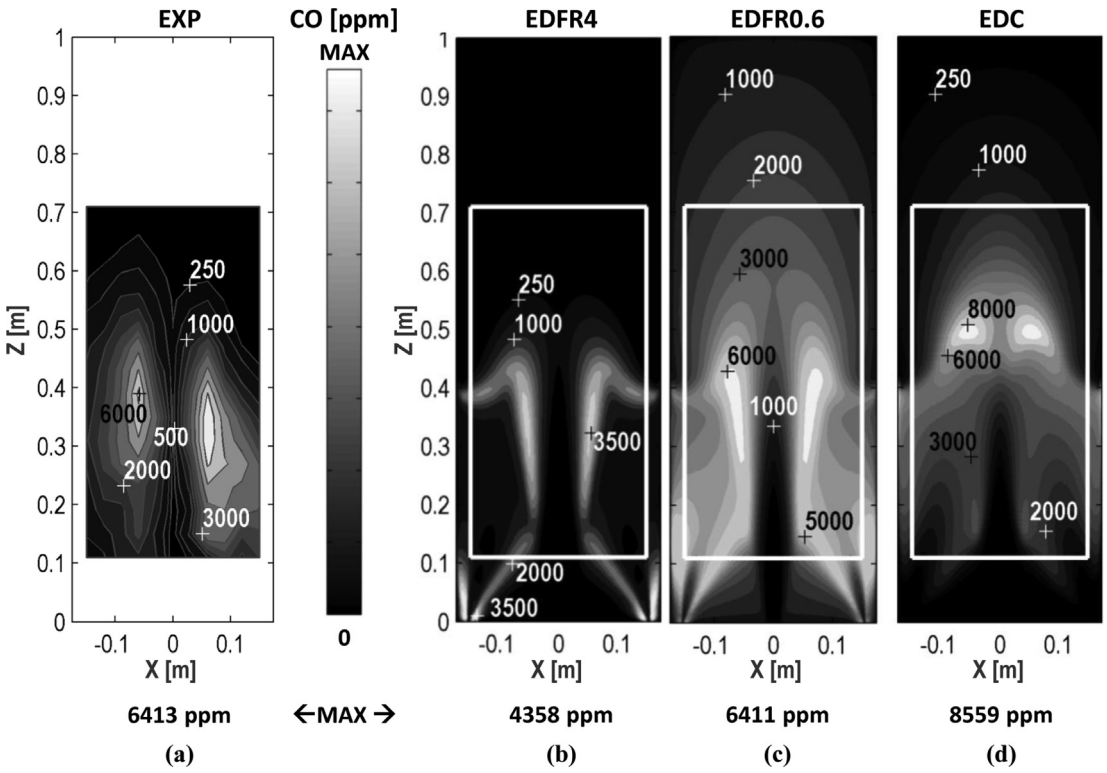

Fig. 7. Experimental (a) and numerical (b, c, d) CO mole fractions (dry basis) in plane (*X*,*Z*) for $E = 20\%$.

Aminian et al. [26] on a jet in hot co-flow modelling, or by testing other reaction mechanisms.

4.2.2. The progress of the reaction

The progress of carbon dioxide production along the air jet axis (*Z* axis) is presented in Fig. 8 for both operating points. The CO_2 mole fraction is normalized by its value at outlet ($X_{CO_2}^*$) to make the comparison easier. The curves obtained from the numerical results with EDFR models are coincident below $Z = 0.3$ m, i.e. the position of the meeting point of air and fuel jets, probably because in this region CO_2 increase is due to dilution. Beyond this point, as the reaction proceeds, the reduction of the constant A has the effect to slow down the increase of CO_2, if compared with its original value. But both EDFR curves are well above the measurement till about $Z = 0.6$ m. For the EDC model, the evolution is quite different with a real delay for CO_2 increase and seems globally more consistent with the experimental evolution.

4.3. The temperature distribution

The temperature distribution measured inside the furnace is presented in Fig. 9a ($E = 10\%$) and Fig. 10a ($E = 20\%$). The experimental fields correctly demonstrate another characteristic of flameless combustion: the temperature uniformity. The difference between the maximum temperature in the furnace and the average wall temperature is around 200 °C for both values of *E*. The position of the maximum temperature is located far from the burner at mid-height of the furnace.

The EDFR models give consistent predictions compared to the experimental results about the shape of the temperature fields; however the maximum temperature levels are overestimated by about 200 °C with the standard EDFR model (Figs. 9b and 10b). With the reduction of the constant A (Figs. 9c and 10c) the maximum temperature reached in the furnace is still 45 °C or 80 °C higher than the. With the EDC model, the maximum temperature

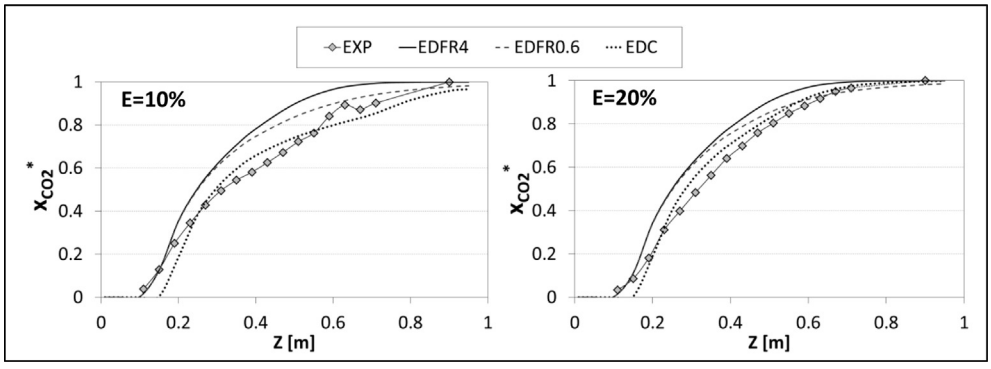

Fig. 8. Progress of the normalized CO_2 mole fraction along *Z* axis.

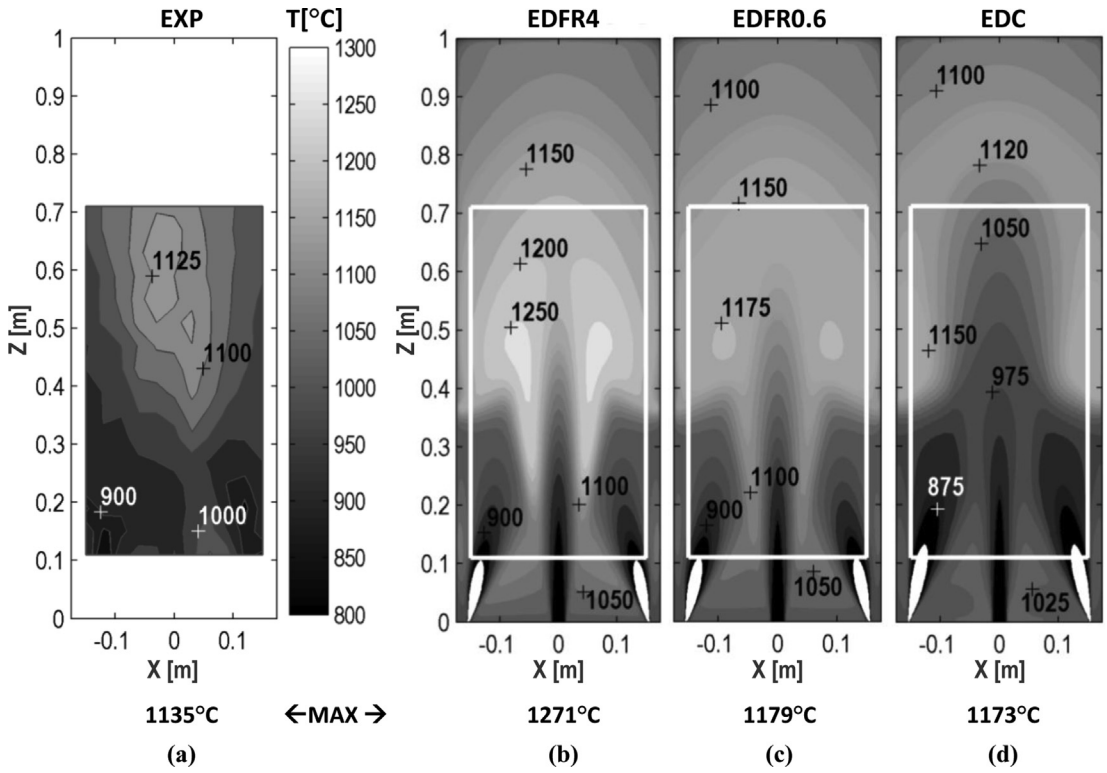

Fig. 9. Experimental (a) and numerical (b, c, d) temperature fields in plane (X,Z) for $E = 10\%$.

level is similar to what is obtained with the EDFR with the reduction of the constant A, but the temperature distribution differs significantly. For $E = 20\%$ (Fig. 10d), the high temperature zone is located farther downstream compared to the results with the EDFR models. For $E = 10\%$ (Fig. 9d), this high temperature zone is lifted downstream of the meeting point of the reactant jets (around $Z = 0.3$ m) and seems to continue within the recirculation zone along the walls as the CO distribution has already shown.

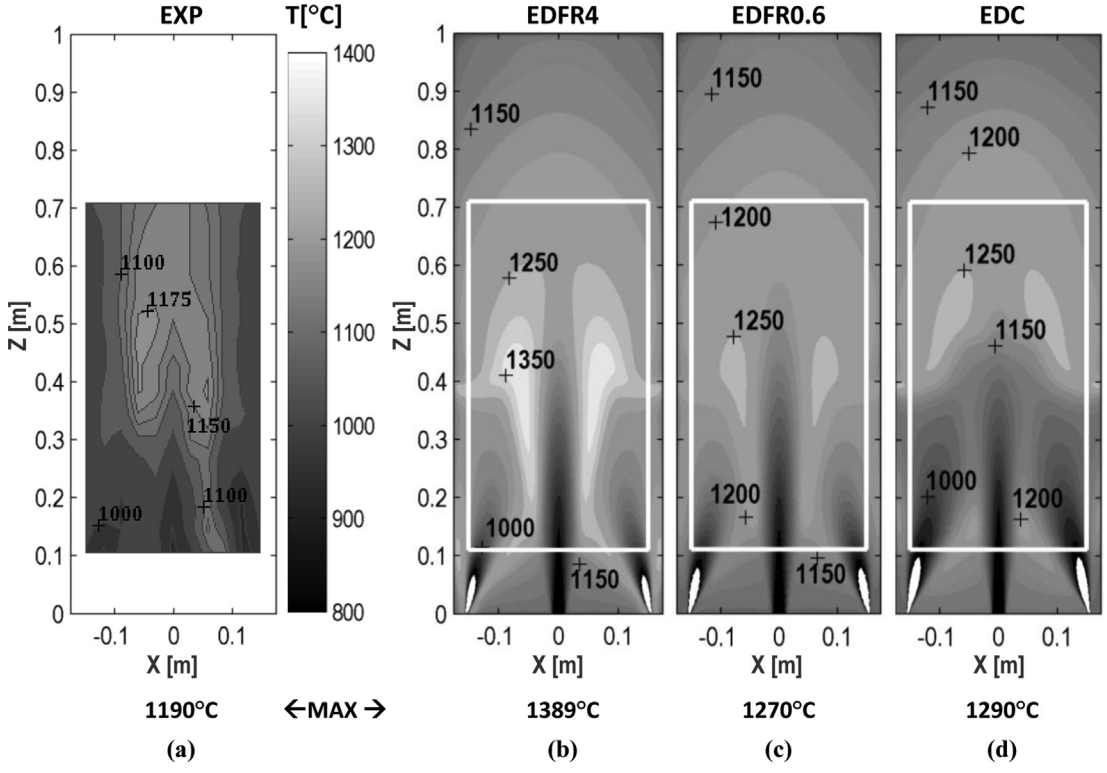

Fig. 10. Experimental (a) and numerical (b, c, d) temperature fields in plane (X,Z) for $E = 20\%$.

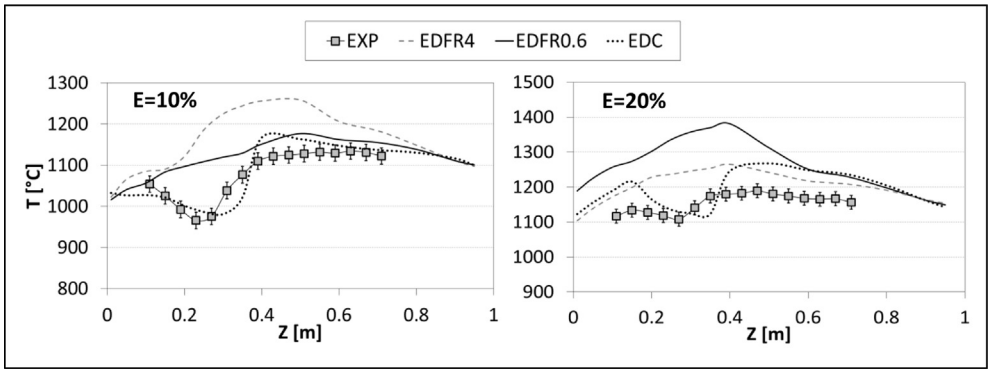

Fig. 11. Maximum temperature in plane (*X*,*Z*) along the *Z* direction.

To compare globally the evolution of the temperature along the furnace, the maximum temperature along the *X* direction for each *Z* position is reported in Fig. 11. Both experimental curves present a minimum around the meeting point of the jets ($Z \sim 0.3$ m) then an increase due to the reaction followed by a fairly constant temperature level around 1135 °C and 1170 °C for $E = 10\%$ and 20%. It is clear that only the EDC model predicts a similar evolution, with an overestimation which is stronger for $E = 20\%$. The EDFR models largely overestimate the maximum temperature throughout the furnace. The reduction of the constant A decreases the maximum temperature level but does not change the shape of the curve.

4.4. NO emissions

The NO emissions at outlet, presented in Table 1 for an equivalent composition of flue gas corresponding to 3% oxygen, are very low as expected in flameless conditions. The EDFR model with the modification of the constant A gives values which are two orders of magnitude below the experimental one. The EDFR model with the standard constant A is not represented in Table 1 due to the large overestimation of the maximum temperature. Only the EDC model gives a good prediction of the NO emission. The increase of the NO production with the excess air observed experimentally is also correctly captured with this model even if the absolute values are a little too high. Considering independently each of the formation routes, it is observed that the N_2O route is responsible for about 95% of the total amount of NO, as already observed by Tabacco et al. [4] and Danon et al. [10]. Since the post processing tool for NO_x computation is the same for both combustion models, the improvement brought by the EDC model is attributed to a better estimation of the O content (and OH for thermal route) thanks to the integration of this radical species in the reaction mechanism while it has to be estimated from chemical equilibrium with the EDFR models.

Table 1
NO mole fraction in flue gas for an equivalent composition to 3% O_2 – Effect of the formation route.

NO@3%O_2 (dry) [ppm]	EDFR0.6		EDC	
	$E = 10\%$	$E = 20\%$	$E = 10\%$	$E = 20\%$
Thermal	1×10^{-3}	1×10^{-2}	0.4	1.6
Prompt	2×10^{-3}	2×10^{-2}	0.04	0.1
Thermal + N_2O	4.6×10^{-2}	0.13	12.5	28.2
Total	**0.05**	**0.14**	**12.6**	**28.3**
Experiment	**5**	**19**	**5**	**19**

5. Conclusion

Detailed experimental data set has been generated in MILD conditions on a laboratory scale furnace with a typical industrial configuration regarding the injection system, the high recirculation level and the presence of a load. The objective was to propose a validation case between fundamental and industrial research, thanks to in-furnace temperature and species measurements with a good spatial resolution.

The RANS modelling of the same furnace is then carried on to assess the performance of the Eddy-Dissipation Concept model (EDC), presented in the literature as one of the most satisfying combustion model in flameless conditions, compared to the more classical Eddy-Dissipation model (EDFR). The EDFR model can be preferred to save computational time as it predicts correctly heat and mass balance and even the temperature peak inside the furnace if the empirical constant A is reduced. The EDC model is the only one which gives the good order of magnitude for NO emission thanks to its ability to include more species in the reaction mechanism among which the intermediate species involved in the NO reaction rate. However, if the order of magnitude and the trend of NO emission with increasing excess air are correct, the absolute value is about twice the experimental value. The analysis of the contribution of each of the formation routes reveals that the N_2O reaction pathway is responsible of as much as 95% of the NO produced in those flameless conditions. The EDC model is also able to capture the impact of the kinetic limitation due to dilution, but the reaction delay is overestimated. As a consequence, the shape and the position of the reaction zone do not fit to experimental observations, even if the effect of the operating conditions is correctly predicted in a relative way. Its high sensitivity to the operating conditions is an asset for flameless modelling, but makes the EDC model more dependent on the turbulence model or the quality of the mesh than the EDFR model.

In conclusion, while its adequacy for MILD combustion modelling is not discussed, the use of the EDC model requires further analysis to be optimized and this cannot be done without the availability of multiple experimental data sets such as the one presented in this paper.

Acknowledgements

The authors wish to thank the Walloon Government for its financial support which allowed the construction and the instrumentation of the laboratory scale furnace.

References

[1] A. Cavaliere, M. Joannon, Mild combustion, Prog. Energy Combust. Sci. 30 (2004) 329–366.
[2] J.A. Wünning, J.G. Wünning, Flameless oxidation to reduce thermal NO formation, Prog. Energy Combust. Sci. 23 (1997) 81–94.
[3] T. Hasegawa, R. Tanaka, High temperature air combustion-revolution in combustion technology-(Part I, new findings on high temperature air combustion), JSME Int. J. 41 (1998) 1079–1084.
[4] D. Tabacco, C. Innarella, C. Bruno, Theoretical and numerical investigation on flameless combustion, Combust. Sci. Technol. 147 (2002) 1–35.
[5] F.C. Christo, B.B. Dally, Modeling turbulent reacting jets issuing into a hot and diluted coflow, Combust. Flame 142 (2004) 117–129.
[6] A. De, E. Oldenhof, P. Sathiah, D.J.E.M. Roekaerts, Numerical simulation of Delft-Jet-in-Hot-Coflow (DJHC) flames using the Eddy Dissipation concept model for turbulence-chemistry interaction, Flow. Turbul. Combust. 87 (2011) 537–567.
[7] M. Mancini, Analysis of Mild Combustion of Natural Gas with Preheated Air, Clausthal University of Technology, 2006 (PhD Thesis).
[8] F. Wang, J. Mi, P. Li, C. Zheng, Diffusion flame of a CH4/H2 jet in hot low-oxygen coflow, Int. J. Hydrogen Energy 36 (2011) 9267–9277.
[9] A. Parente, C. Galletti, L. Tognotti, Effect of the combustion model and kinetic mechanism on the MILD combustion in an industrial burner fed with hydrogen enriched fuels, Int. J. Hydrogen Energy 33 (2008) 7553–7564.
[10] B. Danon, E.-S. Cho, W. de Jong, D.J.E.M. Roekaerts, Numerical investigation of burner positioning effects in a multi-burner flameless combustion furnace, Appl. Therm. Eng. 31 (2011) 3885–3896.
[11] G.G. Szegö, B.B. Dally, G.J. Nathan, Operational characteristics of a parallel jet MILD combustion burner system, Combust. Flame 156 (2009) 429–438.
[12] M. Sánchez, F. Cadavid, A. Amell, Experimental evaluation of a 20kW oxygen enhanced self-regenerative burner operated in flameless combustion mode, Appl. Energy 111 (2013) 240–246.
[13] I. Roiha, J. Kaikko, K. Jaanu, E. Vakkilainen, Analysis of high flue gas recirculation for small energy conversion systems, Appl. Therm. Eng. 63 (2014) 218–226.
[14] A. Rebola, M. Costa, P.J. Coelho, Experimental evaluation of the performance of a flameless combustor, Appl. Therm. Eng. 50 (2013) 805–815.
[15] M. Castela, Veríssimo, A.M.A. Rocha, M. Costa, Experimental study of the combustion regimes occurring in a laboratory combustor, Combust. Sci. Technol. 184 (2012) 243–258.
[16] A. Rebola, P.J. Coelho, M. Costa, Assessment of the performance of several turbulence and combustion models in the numerical simulation of a flameless combustor, Combust. Sci. Technol. 185 (2012) 600–626.
[17] S. Murer, B. Pesenti, P. Lybaert, Characterization of flameless combustion of natural gas in a laboratory scale furnace, in: 2nd Eur. Combust. Meet., Louvain-La-Neuve, Belgium, 2005, p. 253.
[18] D. Lupant, B. Pesenti, P. Lybaert, Influence of probe sampling on reacting species measurement in diluted combustion, Exp. Therm. Fluid. Sci. 34 (2010) 516–522.
[19] I. Ertesvåg, B. Magnussen, The eddy dissipation turbulence energy cascade model, Combust. Sci. Technol. 159 (2000) 213–235.
[20] B.F. Magnussen, B.H. Hjertager, On the mathematical models of turbulent combustion with special emphasis on soot formation and combustion, in: 16th International Symposium on Combustion, Pittsburgh, USA, 1976, pp. 719–729.
[21] M.D. Smooke, Reduced Kinetic Mechanisms and Asymptotic Approximations for Methane-Air Flames, vol. 384, Springer Verlag, New York, USA, 1991, pp. 1–28.
[22] A.A.F. Peters, R. Weber, Mathematical modeling of a 2. 25 MWt swirling natural Gas flame. Part 1: eddy break-up concept for turbulent combustion; probability density function approach for nitric oxide formation, Combust. Sci. Technol. 110-111 (1995) 67–101.
[23] R. Hekkens, M. Mancini, CFD modelling of high efficiency combustion, in: 14th IFRF Member Conference, Nordwijkerhout, Netherlands, 2004 session 5.
[24] D. Lupant, B. Pesenti, P. Evrard, P. Lybaert, Numerical and experimental characterization of a self-regenerative flameless oxidation burner operation in a pilot-scale furnace, Combust. Sci. Technol. 179 (2007) 437–453.
[25] S. Zahirovi, R. Scharler, I. Obernberger, Advanced gas phase combustion models: validation for biogases by means of LES and experiments as well as application to biomass furnaces, in: 7th Conference on Industrial Furnaces and Boilers, Porto, Portugal, 2006, p. 74.
[26] J. Aminian, C. Galletti, S. Shahhosseini, L. Tognotti, Numerical investigation of a MILD combustion burner: analysis of mixing field, chemical kinetics and turbulence-chemistry interaction, Flow. Turbul. Combust. 88 (2012) 597–623.